Vortex streets behind bridge piers - Studies with Telemac-2D/3D & Telemac-AD

Christian Kessler
BERNARD Ingenieure ZT GmbH
Hall, Austria
christian.kessler@bernard-ing.com

Uwe Merkel
UHM River Engineering
Karlsruhe, Germany
info@uwe-merkel.com

***Abstract*— An existing bridge over the Danube River, the longest river in the European Union, will be expanded by two lateral bridges. Four additional bridge piers will potentially induce turbulence, side currents and vortex streets which must not influence the shipping route through and behind the bridge. Simulations with Telemac-2D and Telemac-3D and different pier shapes show Karman vortex streets behind the piers. The ongoing project uses Telemac-3D v7p1 and Telemac-AD to analyze the impact of the piers' shape. The necessary mesh density that is the basis for a reliable representation of the surrounding bathymetry was determined with tests against flume experiments and a mesh impact analysis with Telemac-AD. First results are discussed.**

I. INTRODUCTION

Obstacles in rivers are dangerous for swimmers, sport boats and sometimes even for cargo vessels. Currents near obstacles are different from the mainstream due to changes in fluid elevation, pressure and velocities.

High velocities frequently occur at the lateral face of bridge piers, whereas behind the pier backflow areas, side-currents and vortex streets develop, even if they are not always visible at the surface. At the front-face of an obstacle most of the water moves downward and may draw items down.

The main problem with the simulation of vortex streets is that a good representation is only possible if the mesh resolution is much smaller than the vortex diameters. In the case presented here, the vortex wake will have several hundred meters length, but the average vortex diameters will be below 1 meter at their origin. The necessary mesh resolution has to be small; some experts claim smaller than 1 cm resolution in 3D. But if one needs to simulate a larger river stretch with many bridge piers, a compromise resolution is necessary to keep calculation times acceptable.

Five steps are required to find a suitable mesh with necessary minimum density and to determine good Telemac parameter sets:

1. Straight flume experiments with various pier shapes (circle, ellipse, rectangular a.o.) were set up in different mesh densities. The meshes were programmed to control the mesh point density not only close to the obstacle but also with growing distance.
2. This has been tested with several Telemac setups and compared to classic empiric Kármán formulas for vortex approximations.
3. The mesh points that have an impact on the vortex have been identified with Telemac-AD. This marks the areas that have to be refined carefully.
4. The transfer of these rules to the real river model shows long Kármán vortex streets for academic circular piers and match the empiric formulas.
5. The prediction for the future pier shapes also shows Kármán vortex streets with small vorticity.

II. BOUNDARY CONDITIONS

A. The River and the Bridge

The Danube River (Figure 1) is, after the Volga, the second-longest river in Europe. It is located in central and eastern Europe. Its source is in Germany and the estuary is in Romania where it flows into the Black Sea. The Danube is an important international waterway. Dependent on the flow conditions, ships of up to 195 m in length and a width of up to 22.8 m navigate on the Danube, as do small recreational boats. For all of them strong side currents are a potential hazard.

From the total length of 2,888 km, 2,415 km are navigable, whereby 351 km are located in Austria. This section belongs to the "Upper Danube", which stretches from Kehlheim in Germany to Komárom in Hungary.

Figure 1: Overview of the Danube River

The Voest-bridge (Figure 2), named after the local steel producer, crosses the Danube at river-km 2,133.44. The bridge carries a highway with three traffic lanes and one bicycle lane in each direction. The cable-stayed bridge has one pier, which is permanently in water (Figure 3), on which the approx. 70 m high pylon is located.

Figure 2: Voest-bridge with additional side-bridges 6; project by consortium: Bernard Ingenieure, RWT plus ZT GmbH and Solid architecture.

Figure 3: Voest-bridge with existing bridge piers

There are two more piers in the floodplains; however, these are not of interest for shipping conditions. The shapes and the layout of the existing pier and the new river piers are shown in Figure 4 and Figure 5. The distance between the piers is 130m, which is sufficient space for 2 meeting cargo vessels of the size 195 m x 22.8 m. The free span width on the right side of the pier is approx. 215 m, on the left side approx. 72 m. The distance from pier to slope on the right is 185 m and on the left 60 m.

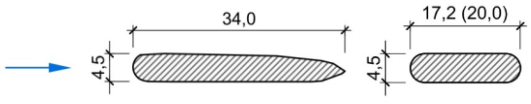

Figure 4: Shape of existing pier - Shape of new piers

In the course of the renovation of the Voest-bridge two additional side bridges will be built. Therefore four additional, new piers will be built in the regular flow section. The effect of the existing pier and the new piers in the regular flow section shall be investigated.

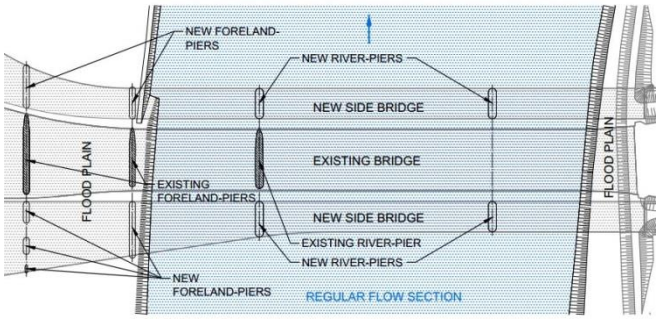

Figure 5: Layout

B. Simulation of Vortex Streets

Based on the research of Theodore von Kármán some empiric formulas and several laboratory examples are available for standard obstacle shapes, mainly for frontal symmetric approaching flow. These formulas, e.g., the vortex creation frequency (1), depend on the Strouhal-number.

$$f = \frac{S_R * V}{d} \qquad (1)$$

where:

- S_R… Is the Strouhal number, approximately 0.2 for the problems discussed in this paper
- V… the steady velocity of the flow upstream of the obstacle
- d… diameter of the obstacle.

The “Body Reynolds Number” (2) influence is well known too, as shown too, as shown in

Figure 6 for the different stages of vortex development.

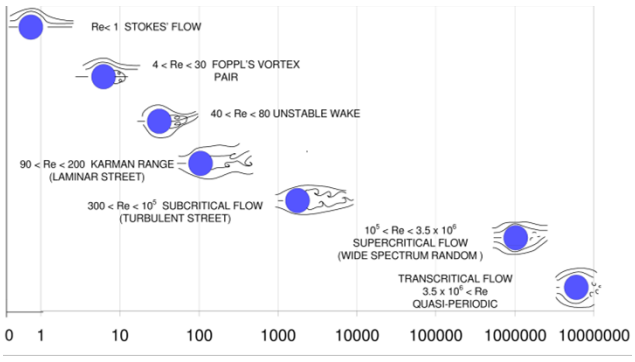

Figure 6: Body Reynolds Number and Vortex Formation [5]

$$\Re = V * d/v \quad (2)$$

where:

- d... the diameter of the cylinder
- V... the steady velocity of the flow upstream of the cylinder
- v... the kinematic viscosity of the fluid.

The separation point of vortices is the point at which the local wall shear stress disappears. Schlichting and Gersten [3] write that the angle of separation for a cylinder under a subcritical flow regime ($300<Re<10^5$) is approximately 80°.

Simulation by finite methods is more challenging to work with than the empiric formulas, as a low diffusion and dispersion is needed to prevent smoothening of the vortices. For Telemac the right advection scheme is known as a key feature. Additionally many scientific publications recommend a very small mesh resolution to keep the dispersion low. Throughout scientific literature, mesh resolution is chosen by the principle "high density, as widespread as the hardware allows us". But it is the nature of these numeric simulations that calculation time and costs are constraints.

The presented simulations in this paper test the abilities of Telemac-3D-v7p1 and Telemac-AD to integrate vortex movements in spatially large, inevitable coarser models.

Contrary to many former tests, the authors use Telemac-AD to quantify the mesh influence point by point in order to not bluntly densify meshes. The intent is to learn where to improve the resolution, where to save mesh points and to reveal unexpected interactions.

III. Tests with Telemac-3D v7p1

A. First tests vs. Observation in Nature

The first simulations of the existing Voest-bridge-piers did not show wake zones. So instead of the genuine shape a circular shape was modelled and consequently wake zones appeared. The question was raised if this is due to numerical reasons, or if there are no wake vortices for non-circular pier-shapes. Therefore the existing Voest-bridge pier and two comparable more non-circular piers at the Inn-river in Innsbruck were photographed and filmed. The results are shown in Figure 7.

All three observations showed wake zones behind the piers. They are not always obvious at first sight, but by studying pictures combined with tripod-filmed videos periodic patterns can be determined. Therefore it is assumed, that the absence of wake zones in simulations is due to numerical reasons.

The Voest-bridge-study covers a 2,900 m long section of the Danube River. The length was chosen based on considerations of calculation time and minimization of boundary conditions influence. The highest navigable discharge in the investigation area is 3670 m^3/s, which was chosen as boundary condition for the numerical simulations. The riverbed friction was defined with a Strickler-coefficient of 37.

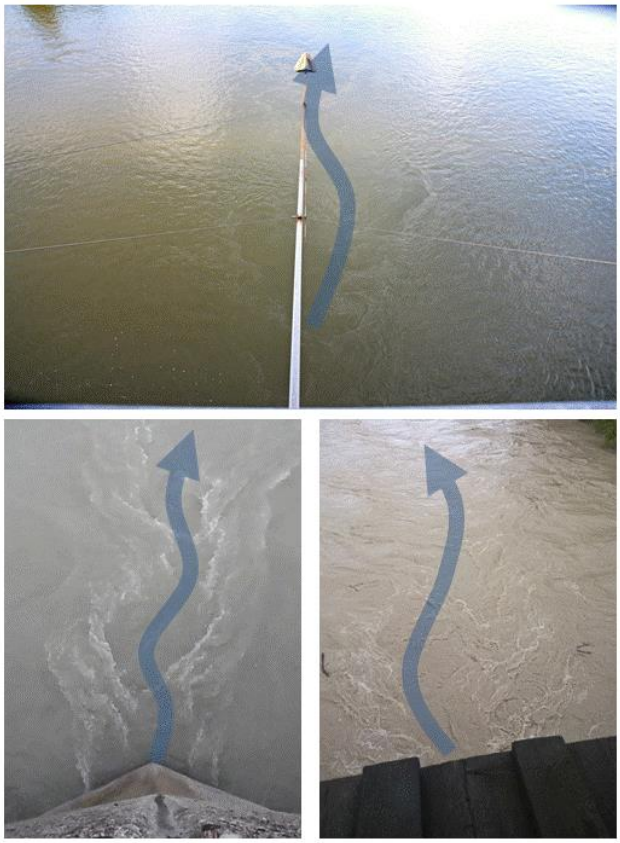

Figure 7: Observation of bridge-piers at the Danube/Voest-bridge (top), Inn-river in Innsbruck (lower-left) and Hall (lower right)

In order to study the effect of the pier, different shapes (Figure 8) were simulated with Telemac-2D v6p3 and v7p1. All parameters which influence the diffusivity were set to reduce it (e.g. velocity diffusivity). The calculation was performed nearly explicit (implicitation for velocity/depth = 0.9) in order to obtain less smoothing. Different advection-schemes and turbulence models with little smoothing were tested.

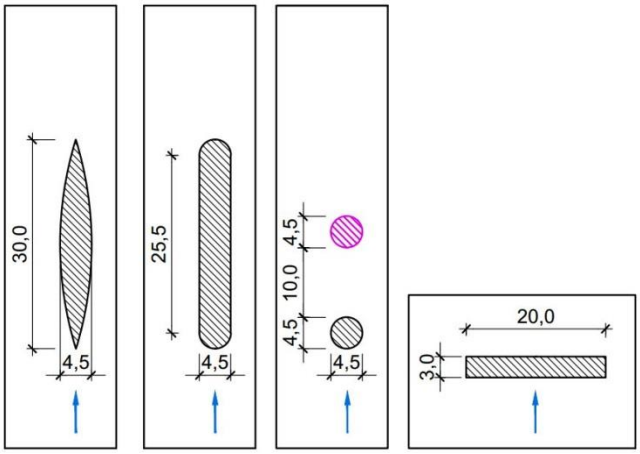

Figure 8: Studied pier shapes and arrangements

The results of the first simulation are shown in Figure 9. It was assumed, that the smoothing comes from dispersion, which is a problem of coarse meshes.

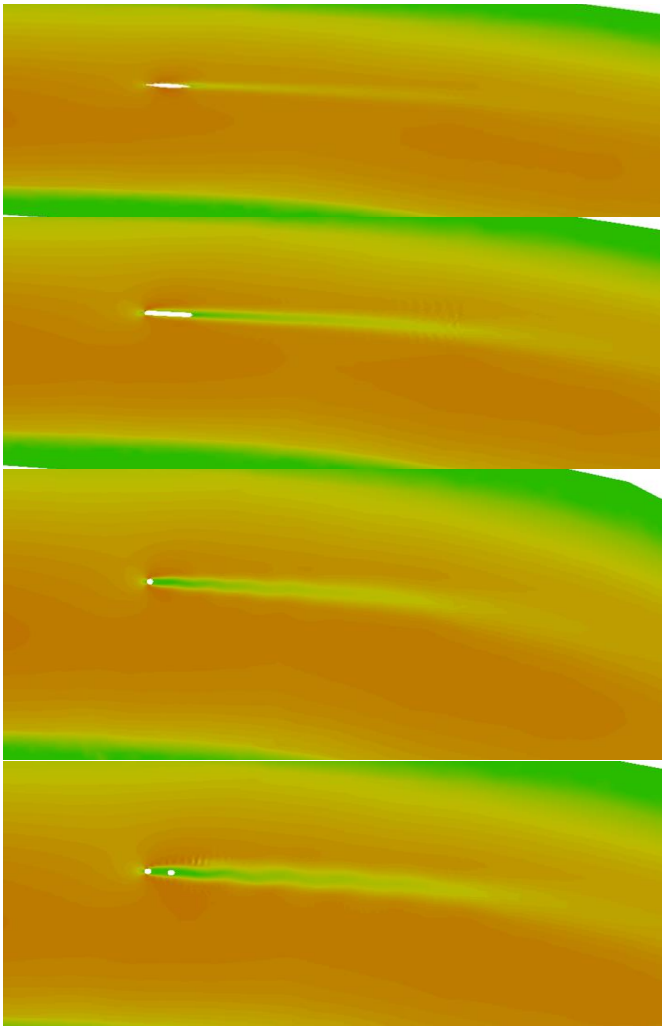

Figure 9: Wake zones vary with the pier shapes, but no Karman vortex streets are visible here.

B. Mesh Dependency and Telemac-AD

Two methods were chosen to find the right mesh / parameter combination:

- Manual densification until there is no further significant change in the results any more
- Selective densification based on Telemac-AD

For the first approach a series of flume meshes had been programmed with a Python script that instrumentalized Jonathan Shewchuk Triangle library [4]. Figure 10 shows meshes for a circle with r=1m and an ellipse with r1=1m and r2=4m. The displayed mesh densities are 180 (upper) and 40 (lower) points at the pier footprint and the triangle growth rate is 1.15 for every ring further away from the center. Despite of being clipped for Figure 10, the length upstream and downstream the pier is 50m, the total width is 20m. The first calculations showed a good vortex production for the circular mesh if used with the advection scheme "weak form of characteristics" and a small implicitation for depth and velocities. The vortex frequency could be reproduced exactly according to the Kármán law: 0.2Hz which equals one new vortex every 5 seconds. Additionally the separation point of vortices fits to Schlichting and Gersten's [3] experience. Figure 11 provides a good impression.

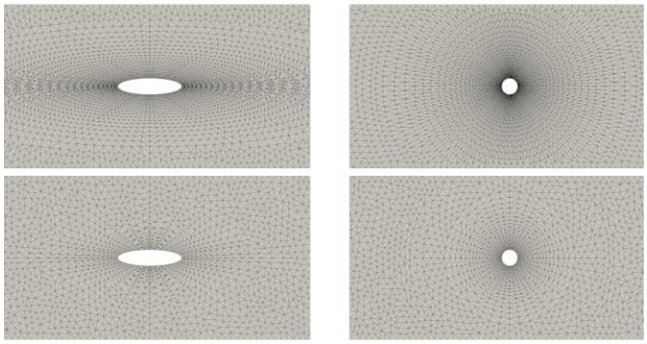

Figure 10: Meshes with controlled point density at the pier and guaranteed point distance growth of less than 1.15 times the neighbouring distance.

Mesh densities with less than 40 points around the circular pier didn't perform well. Starting with 40 points (which equals a boundary point distance of ~15cm) useful results were produced. With 160 points (which equals ~4 cm) the behaviour seemed to reach a tangent. 720 points did not change much, but increasing computational expenses. Therefore brute force densification came to its limits and already included too many nodes.

The second, smarter step was to use Telemac-AD to determine the right positions for high resolution mesh inserts.

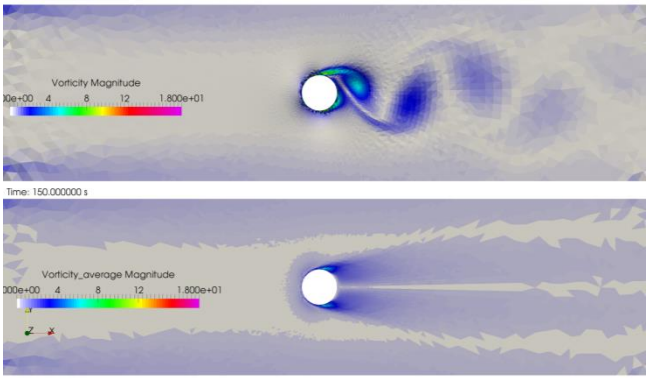

Figure 11: Upper Picture: Estimating vortex zones with the "weak form of characteristics" option produces results that comply with Kármán's formula for the vortex creation frequency. Lower picture: The time averaged vortex corridor.

Telemac-AD (T-AD) is a special sibling of Telemac, which is able to show the interaction between any calculation parameter, as long as it is of the Fortran data type "double precision". In this case, it is the mesh point's position on a user specified result: the vorticity behind the obstacle. The scientific background is explained in more detail in the TUC Proceedings of 2013[2].

T-AD is able to determine the influence of a large number of input variables on one single target variable in a single calculation. This means for the case presented in this paper, that 7,121 points in 2D have X, Y and Z coordinates, which are in total 21,363 variables, which might affect the one result: the vorticity behind the pier.

For this purpose a so called *cost function* is added to the Telemac Source code, like an internal post processing routine.

After every time step it processes a formula which quantifies the vorticity behind the pier. Several alternative cost functions were checked. The most useful among them were the standard deviation of the velocity components, the variability of U_y and the transfer velocity component. Figure 12 shows an orange frame which marks the examination zone for the displayed cost function. In Figure 13 this is the smaller purple zone.

T-AD v6p2 and v7p2 (so far unpublished) returned the adjoints (~ a kind of derivative) for the mesh variables X, Y and Z which are combined to generate the vector field (=arrows) in Figure 13. The arrows describe the direction and magnitude a mesh point should be shifted to increase the vorticity indicator (=cost function).

Note: This answer is the elementary input for a potential next step, the shape optimization. In the case presented here it means that if the Y-dimension of the pier would be bigger, the vorticity indicator would be stronger.

To return to the general question of "Which mesh point has influence on the vorticity and therefore needs to be treated with special care?"; in Figure 13 the adjoints' magnitude is colored as an answer. The logarithmic scale might mislead the interpretation. Boundary points have the greatest impact on the results, but the position of the inner points nearby (which are more numerous and cover a larger area) also have an impact on the results. This means, that the mesh dependency is still strong in an area of up to 50 % of pier radius or 50 cm away from the boundary nodes, even though the resolution is already < 6 cm in this zone. This means the initial recommendation was correct: cells have to be smaller here for scientific applications.

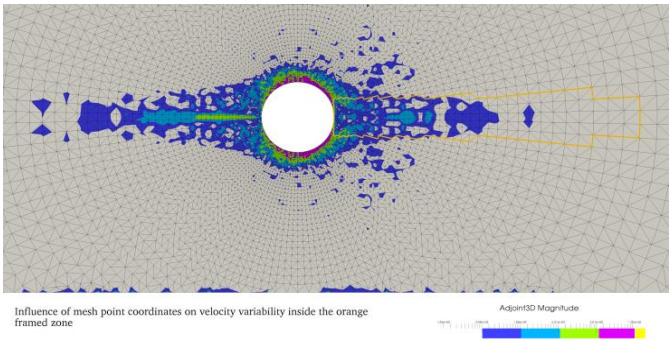

Figure 12: The magnitude of point coordinate adjoints clearly shows the dependency of the vorticity to non-boundary points. This means that shifting one of the coloured points in 2D will lead to slightly other results. Due to the logarithmic scale, the pink coloured boundary points have a 100 times stronger impact than the blue coloured surroundings. However, the blue area is up to 100 times larger.

Another interesting fact is the long influence zone directly upstream of the pier. The sensitivity of this area explains why fins or plates can disturb or even destroy the vortex system that efficiently.

Interpretation for the potential linear shift of an inner mesh point: As the bottom elevation is 0m for all points, the shift in X and Y direction wouldn't affect the bathymetry, but only the calculated velocity gradients close to the obstacle.

This obviously has no linear behavior and means that a different mesh point position would result in different velocity fields. More points would describe the V-field better, thus resulting in less impact for the single points.

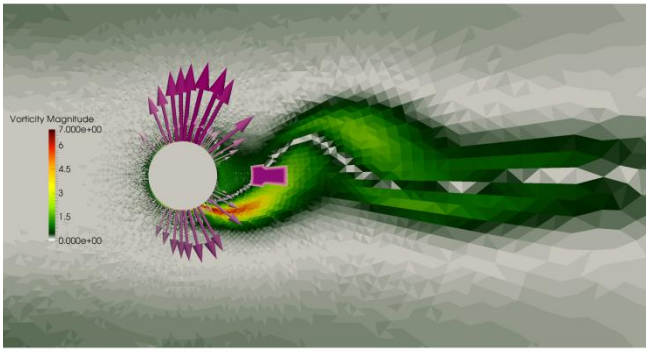

Figure 13: If the adjoints are displayed as arrows, they show the direction a mesh point has to be moved to increase the vorticity inside the pink selected area. The opposite direction would reduce it. In particular, the direct boundary points give the expected answer: Shift them to the inner side, and the vorticity will be reduced.

For practical purposes, the smaller differences of the results allow the authors a 15 cm resolution for the final flume-mesh. To understand why the upstream zone around the pillow is still that sensitive for the downstream vortex zone, Figure 14 (Telemac 3D-v7p1, here: 10 Levels in 3D) gives a visual explanation: The impact pillow on the upstream face and the side rolls are clearly visible and separated from the surrounding flow. The downward rotation is strongest at a distance of more than 0.5m to the obstacle itself. Outside of this zone, the impact (as calculated with Telemac-AD) decreases to a negligible magnitude.

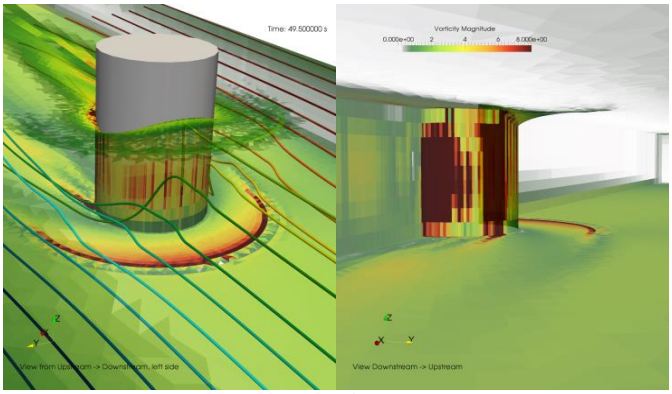

Figure 14: The pillow on the upstream face produces a strong downward drag with the strongest vorticity on the bottom and on the piers back. A fine mesh resolution is necessary for this area as well, as it is an essential component of the vortex building system. The downward drag starts up to 1m before the pier.

After many more comparisons between meshes, empirical formulae and literature, the step to the real scale model was made with the decision towards a mesh size of approx. 10cm along the circular piers rising by a factor of 1.15 to the next ring of cells. The first test with a circular pier returned the expected Kármán vortex street. The frequency is 0.035Hz, which equals the creation of one vortex every 28s. See fig. 15.

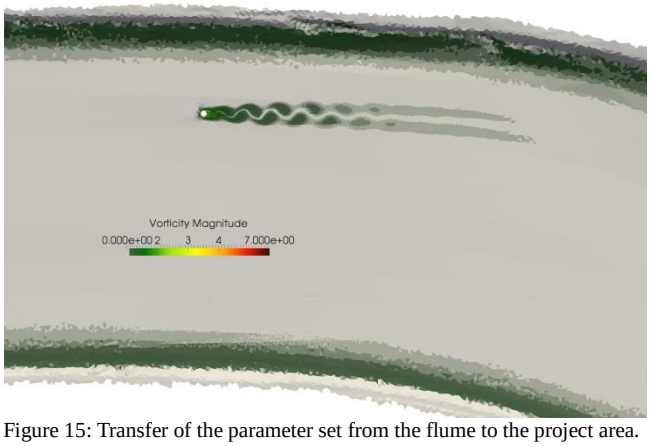

Figure 15: Transfer of the parameter set from the flume to the project area. The resulting vortex street complies with the empirical Kármán formulas.

The next step is the creation of the final mesh. It includes all 5 piers and uses the so far developed parameter setup and mesh densities, but there are no comparison values available anymore from literature or experiments.

With an further mesh-refinement to 5 cm edge length Kármán vortex streets with a small vorticity occur (Figure 16).

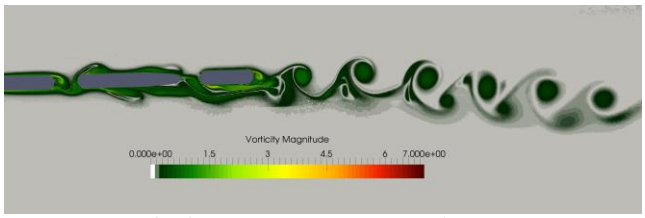

Figure 16: Kármán vortex streets at the piers of the Voest-bridge.

There are more questions to solve: What is the impact of diffusion? And what is the impact on small sport ships? At the time of writing, the answers to these questions are open, but we will publish some more results and a downloadable Telemac-AD example on the webpage

www.uwe-merkel.com/piers-and-eddies

IV. CONCLUSION

Vortex streets can be modeled well enough to comply with the well validated empirical formulas. It is important to avoid anything that induces artificial diffusion / dispersion. Two significant sources of dispersion are known beside some smoothing parameters: The mesh density and the type of advection. For the latter, the “weak form of characteristics” is the best possible answer in Telemac v7p1. For the first, the mesh density, the authors have not yet derived a universal empirical formula. However, in general results improved and met the Kármán frequency, when:

- the smallest cross section of the upstream pillow was resolved by at least 5 to 7 cells.
- and this resulting point density was used over a zone which starts at approx. 5 times the pier width before the pier until 10 times the width after the pier
- the triangle growth rate was kept <. 1,15
- the Delaunay criteria for the triangle shape was kept strictly
- the Courant-Friedrich-Levy criteria < 1 for the time step was kept.

Telemac-AD proved itself to be a reliable influence detection tool. It is particularly useful for more sophisticated pier shapes or groups (especially beyond the standard circular, elliptical, arrow or rectangular shapes).

Further parameters, such as resulting shear stress or scour development have not been investigated. Further fine-tuning will be necessary to meet the accuracy demands of the latter.

The width and dissipation of the wake is also mesh dependent, but in general less sensitive to the tested parameters.

ACKNOWLEDGEMENT

We thank Jan Riehme for the support on Telemac-AD and his work on it.

Further we thank the Amt der Oberösterreichischen Landesregierung, the Via Donau and the ASFINAG for their permissions and data.

REFERENCES

[1] ASFINAG. 2016. Neugestaltung Voestbrücke. Download 21.09.2016. www.asfinag.at

[2] Merkel, U. Riehme, J. 2013. Reverse engineering of initial & boundary conditions with TELEMAC and algorithmic differentiation. In: Proceedings – Telemac Users Club 10 / 2013, Karlsruhe

[3] Schlichting H. Gersten K. 2000, Boundary Layer Theory, 8th rev. and enl. ed., Springer, Berlin

[4] Shewchuk, J. R. Delaunay Refinement Algorithms for Triangular Mesh Generation, Computational Geometry: Theory and Applications 22, May 2000

[5] Xanthakos, P. 1995. Bridge Substructure and Foundation Design, Prentice Hall PTR, New Jersey